

# Single Electron Measurement in the $d+Au$ Collisions at $\sqrt{s_{NN}} = 200$ GeV

F. Kajihara, Y. Akiba<sup>a</sup>, R. Averback<sup>b</sup>, S. Butsyk<sup>b</sup>, H. Hamagaki, K. Ozawa, T. Tabaru<sup>c</sup>,  
M. Togawa<sup>d</sup>, and X. Wei<sup>c</sup> for the PHENIX Collaboration

Center for Nuclear Study, Graduate School of Science, University of Tokyo  
<sup>a</sup>RIKEN (The Institute of Physical and Chemical Research)

<sup>b</sup>Department of Physics and Astronomy, Stony Brook University, SUNY, USA

<sup>c</sup>RIKEN, BNL Research Center, Brookhaven National Laboratory, USA

<sup>d</sup>Department of Physics, Kyoto University

## 1. Introduction

Heavy-quark (charm and beauty) measurements provide valuable information for testing perturbative QCD (pQCD) predictions [1]. The measurements should impose stringent limitations on uncertainties in the Leading Order (LO) and the Next-to-Leading Order (NLO) pQCD calculations of heavy-quark productions which considerably depend on the gluon distribution function because heavy quarks are mainly produced *via* gluon fusions [2]. In heavy-ion collisions, non-pQCD effects, such as cold nuclear effects can also modify the gluon distribution. Since such nuclear effects are unknown in high-energy region, it is important to investigate these influences on the heavy-quark yield.

Heavy-quark production also has an important role in the investigation of the hot and dense matter created in heavy-ion collisions. The heavy-quark momentum spectrum may be affected by final state interactions such as its energy loss in the dense medium. On the other hand, energy loss of heavy quarks with a certain momentum is predicted to be smaller than that of light quarks with the same momentum due to the larger quark mass [3,4]. The measurement of heavy quarks with momentum will verify the flavor dependence of energy loss. For precise measurements, it is essential to estimate properly the contributions from the above-mentioned nuclear effects. Data from the RHIC-PHENIX experiment of  $d+Au$  collisions at  $\sqrt{s_{NN}} = 200$  GeV in 2003 (called Run-3) is suited to study the cold nuclear effects, since no high-energy-density matter is formed.

The measurement of single electrons ( $e^+$  or  $e^-$ ) from semi-leptonic decays of heavy quarks is a useful way to study heavy-quark production. Inclusive electrons can be categorized into two groups. The first group consists of "photonic" electrons mainly from (1) Dalitz decays of mesons ( $\pi^0$ ,  $\eta$ , etc) and (2) photon conversion. The second is termed "non-photonic" electrons. The decays of charm and bottom are the dominant sources of the second group. This report presents the status of the *non-photonic* electron measurements in the Run-3  $d+Au$  experiment.

## 2. Electron Measurement in the PHENIX

In the PHENIX experiment, electron measurements are performed using two central arm spectrometers. Each arm is composed of a Drift Chamber (DC), Pad Chambers (PC), a Ring-Imaging Čerenkov counter (RICH) and Electro-Magnetic Calorimeters (EMCal), covering pseudo-rapidity

$|\eta| < 0.35$  and  $\pi/2$  in azimuth ( $\phi$ ) [5]. The PHENIX Minimum Bias (MB) trigger information is generated using two Beam-Beam Counters (BBC) which are placed at  $\pm 145$  [cm] from the center of the PHENIX along beam axis ( $z$ ). The BBC provides measurement of centrality and vertex position, too. The DC measures charged particles trajectories in  $r - \phi$  direction to determine  $p_T$  of the particles. The PC provides 3-D spatial point measurement for tracking of charged particles and longitudinal momentum reconstruction in combination with the DC hit information. The RICH and EMCal are main detectors to identify electrons in the PHENIX. The RICH detects the Čerenkov light which only electrons produce in its CO<sub>2</sub> radiator (1 atm) below 4.9 GeV/c (Čerenkov threshold momentum of charged pions). The EMCal can measure deposited energy and spacial positions of the electromagnetic showers by electrons. The RICH and EMCal form an electron trigger system, called the EMCal-RICH Trigger (ERT) [6]. To evaluate the ERT efficiency for electrons, a trigger simulator was developed in the PHENIX simulation framework.

## 3. "Converter Subtraction" Method

To extract *non-photonic* electron yield  $N(p_T)$  by subtraction of *photonic* electron yield  $P(p_T)$  from the total, the "converter subtraction" method is applied [7]. In the Run-3, special runs were performed with a photon converter, made of a brass sheet (1.68 % radiation length) around MVD (see the reference [5]). The photon-converter can enhance  $P(p_T)$  by a certain factor  $R_\gamma$  since the internal (virtual) and external (real) photon conversion in the above (1) and (2) have a similar form factor with dependence of radiation length. Here,  $R_\gamma$  means the ratio of *photonic* electron yields with and without the converter. The measured inclusive electron yield  $I(p_T)$  can be expressed as  $I(p_T) = P(p_T) + N(p_T)$  without the converter and  $I'(p_T) = R_\gamma P(p_T) + N(p_T)$  with the converter.  $N(p_T)$  is given by these two equations.

## 4. Photonic Electron Simulation

In the converter subtraction method, the evaluation of  $R_\gamma$  is the most important issue. A GEANT based Monte Carlo simulation is used to estimate how much the *photonic* electron yield is increased by the photon converter and determine  $R_\gamma$ . The simulation was performed using the PHENIX-CCJ (Computing Center in Japan) and RIKEN

Super Combined Cluster (RSCC).

The source of *photonic* electron in real data is a mixture of mesons ( $\pi^0$ ,  $\eta$ ,  $\eta'$ ,  $\omega$  and  $\phi$ ) decaying into real or virtual photons with their different  $p_T$  slopes. However, contributions from  $\pi^0$  and  $\eta$  occupies almost of all (Table 1). Therefore, *photonic* electrons from only  $\pi^0$  and  $\eta$  were studied in the simulation. The  $R_\gamma$  of  $\pi^0$  ( $R_\gamma^{\pi^0}$ ) and the  $R_\gamma$  of  $\eta$  ( $R_\gamma^\eta$ )

Decay Mode	Branching Ratio of Each Meson
$\pi^0 \rightarrow 2\gamma$	$98.798 \pm 0.032 \%$
$\pi^0 \rightarrow \gamma e^+ e^-$	$1.198 \pm 0.032 \%$
$\eta \rightarrow 2\gamma$	$39.43 \pm 0.26 \%$
$\eta \rightarrow \gamma e^+ e^-$	$0.60 \pm 0.08 \%$
$\omega(782) \rightarrow \pi^0 e^+ e^-$	$(5.9 \pm 1.9) \times 10^{-4}$
$\eta'(958) \rightarrow \gamma e^+ e^-$	$< 9 \times 10^{-4}$
$\phi \rightarrow \eta e^+ e^-$	$(1.15 \pm 0.10) \times 10^{-4}$

Table 1: Main electron decay channels of light mesons. [8]

were determined separately. Then, the  $R_\gamma$  can be determined by combination of the  $R_\gamma^{\pi^0}$  and  $R_\gamma^\eta$ , which is mentioned below. For the original  $\pi^0$  and  $\eta$  spectrum, we used the MB  $p_T$  distributions measured in Run-3 d+Au collisions (the  $\pi^0$  spectrum was published as the reference [10]).

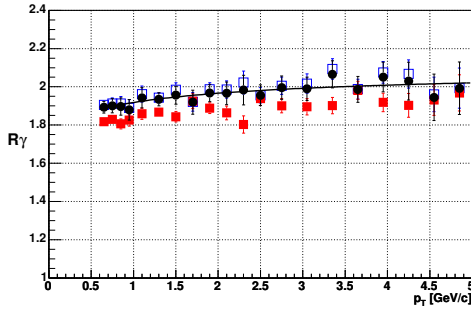


Figure 1: Combined  $R_\gamma$  (closed circle) of  $R_\gamma^{\pi^0}$  (open square) and  $R_\gamma^\eta$  (closed square). The solid line is a fitting curve of the combined  $R_\gamma$ .

Figure 1 shows combined  $R_\gamma$  (closed circle) of  $R_\gamma^{\pi^0}$  (open square) and  $R_\gamma^\eta$  (closed square). Since the  $\eta$  mass is larger than  $\pi^0$  mass, the phase space of  $\eta$  Dalitz decay is slightly larger than that of  $\pi^0$  Dalitz decay. The relative branching ratio: (Dalitz decay)/(two  $\gamma$  decay) is 1.2 % for  $\pi^0$  and 1.5 % for  $\eta$ . This difference makes  $R_\gamma^\eta$  smaller than  $R_\gamma^{\pi^0}$ . The combined  $R_\gamma$  is determined as the following expression:

$$R_\gamma = \frac{R_\gamma^{\pi^0} \cdot N_e^{\pi^0} + R_\gamma^\eta \cdot N_e^\eta}{N_e^{\pi^0} + N_e^\eta} = \frac{R_\gamma^{\pi^0} + R_\gamma^\eta \cdot \epsilon^{\eta/\pi^0}}{1 + \epsilon^{\eta/\pi^0}}. \quad (1)$$

$$\epsilon^{\eta/\pi^0} = N_e^\eta / N_e^{\pi^0}. \quad (2)$$

In the above expressions,  $N_e^{\pi^0}$  is a number of electrons from  $\pi^0$  decays.  $N_e^\eta$  is a number of electrons from  $\eta$  decays.  $\epsilon^{\eta/\pi^0}$  is a ratio of  $\eta$  and  $\pi^0$  particle compositions. Since the uncertainty of  $\eta/\pi^0$  ratio ( $0.45 \pm 0.1$ ) is not small, three kinds of spectra were calculated in the cases of  $\eta/\pi^0 = 0.35, 0.45$  and  $0.55$ . The  $\eta/\pi^0$  dependence of the combined

$R_\gamma$  was checked within 0.5 % fluctuations. The value was assigned as systematic error.

## 5. Non-photonic Electron Yield

Figure 2 shows Run-3 d+Au  $N(p_T)$  (close square) which is calculated based on the result of *photonic* electron simulation. Each error bar indicates only statistic error and each square in background shows systematic error as described in Fig. 2. The yield is fully corrected for the trigger efficiency, geometrical acceptance, reconstruction and eID efficiency (see [9]). The spectrum is normalized with binary collision cross section by scaling with  $\sigma_{pp}/(N_{coll} = 8.5)$  for MB triggered event to compare with the *non-photonic* electron spectrum in the Run2 p+p. The spectra in Fig. 2 show no strong nuclear modification. The d+Au spectrum is slightly enhanced around  $p_T = 1.0$  GeV/c, which may indicate *Cronin* effect even in charm production.

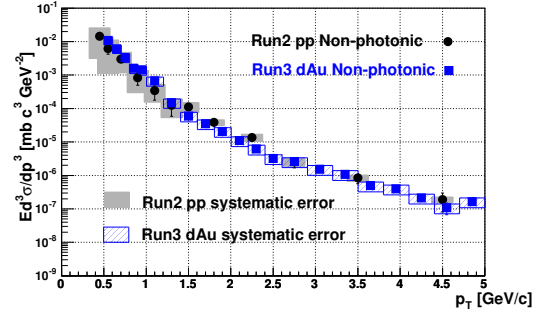


Figure 2: The *non-photonic* invariant cross section as a function of  $p_T$  per binary N-N collision cross section by scaling with  $\sigma_{pp}/(N_{coll} = 8.5)$  for MB triggered event in d+Au collisions (closed square: Run-3 d+Au, closed circle: Run2 p+p).

## 6. Summary and Outlook

*Photonic* electron simulations were performed with high statistics to determine  $R_\gamma$  and its uncertainty. The analysis of *non-photonic* electrons in the high- $p_T$  region ( $\geq 5$  GeV/c) is in progress. The analysis is important for the study of  $b$  quarks. We started to analyze data in the Run4 Au+Au at  $\sqrt{s_{NN}} = 200$  GeV. The statistics is more than 20 times as that used in Run2 Au+Au analysis [7]. Significant reduction of statistical error is expected with these data.

## References

- [1] S. Frixione *et al.*, hep-ph/9702287, (1997).
- [2] R. Vogt *et al.*, Z. Phys. C **71**, 475, (1996).
- [3] S. S. Adler *et al.*, Phys. Rev. Lett. **91**, 072301, (2003).
- [4] Y. L. Dokshitzer *et al.*, Phys. Lett. B **519**, 199, (2001).
- [5] K. Adcox *et al.*, Nucl. Instrum. Methods. A **499**, 469, (2003).
- [6] F. Kajihara *et al.*, CNS Annual Report 2003, 49, (2004).
- [7] S. S. Adler *et al.*, Phys. Rev. Lett. **94**, 082301, (2005).
- [8] K. Hagiwara *et al.*, Phys. Rev D **66**, 010001 (2002).
- [9] F. Kajihara *et al.*, CNS Annual Report 2003, 51, (2004).
- [10] S. S. Adler *et al.*, Phys. Rev. Lett. **91**, 072303, (2003).